



African Journal of Biological Sciences



Heavy metal ions contaminants removal from industrial waste water stream *via* using Zinc oxide nanoparticles (ZnO-NPs)

Gajendra Singh Lodhi^a, Jyoti Sharma^{a*}, Laxman Singh^b

^aDepartment of Chemistry, School of Basic and Applied Sciences, Shobhit Institute of Engineering and Technology (Deemed-to-be-University), Meerut, UP, India- 250110.

^bDepartment of chemistry, Faculty of Science, Siddharth University, Kapilvastu, Siddharth Nagar, UP, India- 272202.

*Corresponding authors: lodhigajendra8@gmail.com (Gajendra Singh Lodhi), drjyotisharma24@gmail.com (Dr Jyoti Sharma).

Abstract

In this recent research article, zinc oxide nanoparticles (ZnO-NPs) were successfully synthesized using the conventional hydrothermal technique. The present study determined comprehensive characterization of metal oxide-based nanoparticles and adsorption efficacy for heavy metal ions. X-ray diffraction (XRD) and Fourier transform infra-red (FT-IR) spectroscopy confirm alteration in the specific functional group and hexagonal structures within the synthesized ZnO-NPs. Furthermore, N₂ adsorption-desorption methodology application achieved a substantial 26.777m²/g surface area, as it accurately demonstrates with the Brunauer-Emmett-Teller (BET) analyzer. Additionally, the SEM-EDX analytical technique is employed to address the ZnO-NPs and heavy metal ions interactions, revealing a promising insight. Although, the batch adsorption kinetic experiment expresses a higher degree affinity of ZnO-NPs for cupric ions (Cu²⁺) compared to chromium (Cr³⁺), lead (Pb²⁺) and nickel (Ni²⁺). The maximum adsorption capacity (88.547 mg/g) was attained at optimal conditions (pH 4, 1 g/l adsorbent dose, 250-minute contact time and 50 mg/l initial Cu²⁺ ion concentration). Furthermore, the adsorption process illuminates chemisorption mechanism, which point out the monolayer type removal of heavy metal ions, as evidently confirms with pseudo-second-order kinetics model. The present study shows the potential of ZnO-NPs in eradicating positively charged heavy metal ions, particularly Cu²⁺ ions, from contaminated wastewater streams. This study findings advocate in a full support to the metal oxides-based nanomaterials, an outstanding role in the purification of contaminated wastewater.

Keywords: Nanoparticles, ZnO-NPs, adsorption, heavy metal ions (Cu, Cr, Pb, Ni) and mechanism of action.

Article History

Volume 6, Issue 5, 2024

Received: 09 May 2024

Accepted: 17 May 2024

doi: 10.33472/AFJBS.6.5.2024.5565-5581

Introduction

Heavy metal ions are accumulated in living organisms in an unregulated fashion and stored in an excess than excreted amount as a result of consequences of human population growth and industrialism. It also leads to a constant depletion of natural resources especially fresh water resources with the dumping of agri-waste, domestic, industrial waste in an uncontrolled manner. Among these metal ions, copper ion (Cu^{2+}) is one of the most abundant pollutants in waste water (Ali et al., 2016) on account of wide scale applications in number of sectors such as electroplating industries (He et al., 2019), agricultural processes, welding process, agricultural processes, plumbing and electrical materials [1,2]. Bio-accumulation of copper (Cu^{2+}) ion consumption in high rate causes a number of harmful human disorders, which affect the normal functioning of main organs such as liver, kidney, brain and lung (Saleh, 2017; Kushwaha and verma,2017) [3,4]. Thus, conservation of our environment and human health is of utmost importance to eradicate the problem of copper (Cu^{2+}) ion from industrial waste water before disposed off into main stream of water. However, discharge water cleaning can takes place possibly by means of chlorination (Al-Abri et al., 2019), ultraviolet and ozonation are widely known conventional methods (Bandyopadhaya, 2016) [5,6]. However, these highlighted conventional methods have several major challenges. Chlorination for instance, is ineffective against resilient water-borne pathogens and can produce carcinogenic byproducts when chlorine is added into polluted water streams. Ozonation is a costlier alternative option and forms bromate when ozone (O_3) reacts with bromide ions in wastewater. Ultraviolet treatment is a vital in this sense, while leaving no residual materials in water streams after treatment, provides no protection against the possibility of re-infection within the distribution network as suggested by Environment Protection Agency (EPA, 2011).

In the realm of environmental remediation, several advanced chemical technologies have been explored and utilized to remove copper ions from waste water (Fu and Wang, 2011), including precipitation (Negrea et al., 2008), electrocoagulation (Dermentzis et al., 2011), filtration (Kebria et al., 2015) and ion exchange (Dąbrowski et al., 2004) [7-11]. However, these highlighted techniques are often inefficient and expensive when these are selected to eliminate trace amount of heavy metals.

In this context, adsorption emerges as a popular method for its cost-effectiveness, ease of use, (Rafiq et al., 2014; Ali et al., 2016) and recyclability of adsorbents, making it a viable approach to eradicate even a trace-level of metallic ions in wastewater streams [12]. Consequently, newer

approaches based on adsorption phenomena are needed to be explored in order to enhance the efficiency of trace heavy metal ion removal.

This research focuses on the utilization of ZnO nanoparticles as an adsorbent for removing heavy metal ions (Wang et al., 2013a) [13]. Zinc oxide nanoparticles offer low toxicity, biocompatibility, long-term stability (Talaiekhosani et al. 2019; Babu et al. 2019) and ease of reproduction [14,15]. (Leiva et al. 2021) reported that ZnO-NPs have an ability to absorb heavy metal ions *via* hydroxyl groups (-OH) present in wastewater [16]. Numerous researchers have extensively studied the maximal removal of heavy metal ions under optimized environmental conditions using ZnO-NPs, yielding varying conclusions.

This article delves into the adsorption process, selectively employing ZnO-NPs to remove prominent metal ions and assess their adsorption capacities. Furthermore, it examines the impact of various optimal conditions, such as ionic strength, pH, initial concentration, contact time, and adsorbent doses on the adsorption phenomenon. The study reveals the significantly higher affinity of ZnO-NPs for metallic ions in industrial waste water, shedding light on their potential as an effective solution for environmental remediation.

1. Materials and Methods

1.1 Chemical reagents supplied

The Merck India Pvt. Ltd delivered a range of chemicals including sodium hydroxide (NaOH), Zinc acetate dehydrate $\text{Zn}(\text{CH}_3\text{COO})_2 \cdot 2\text{H}_2\text{O}$, Copper nitrate $\text{Cu}(\text{NO}_3)_2$, Nickel nitrate $\text{Ni}(\text{NO}_3)_2$ and Lead nitrate $\text{Pb}(\text{NO}_3)_2$ for conducting this research work. The purchased chemical compounds were of high purity and analytical grade quality in order to ensure the highest level of reproducibility and accuracy in our research results.

1.2 Methods

1.2.1 ZnO-NPs synthesis

ZnO-NPs powder was prepared using a previously reported hydrothermal method. In the initial phase, $\text{Zn}(\text{CH}_3\text{COO})_2 \cdot 2\text{H}_2\text{O}$ was added into absolute ethyl alcohol, and then dispersed into NaOH solution at a molar ratio of 1:2 with continuous stirring at 400 rpm for 30 mins to achieve a uniform solution. Subsequently, the prepared reaction mixture was transferred into a Teflon-lined autoclave at 110 °C for 5 h for sterilization purposes. The samples were kept for cooling at room temperature; the resulting solution was subjected to centrifugation. The precipitate was

then washed thoroughly with distilled water and ethanol, and the resulting white products was dried at 60°C for 24 h.

2.2.2 ZnO-NPs Materials characterization

The structural characterization of ZnO-NPs was conducted with the help of high resolution and powered wider angle-X-ray diffractometer, with scanning at a rate of 4° per min over the 5° to 80° (2θ) range. The FTIR spectra was acquired using a FT-IR spectrometer (Thermo Scientific Nicolet (iS10) employing the KBr pressed disc method, covering a spectral range starting from 500 to 4000cm⁻¹ to analyze the presence of surface functional groups. The surface texture and elemental analysis of the synthesized ZnO-NPs were carried out with scanning electron microscopy coupled with energy dispersive-X-ray spectroscopy (SEM-EDX) in the absence or presence of heavy positive metal ions. However, other peculiar chemical properties such as surface area and pore size distribution measurement of ZnO-NPs were explored through the nitrogen based adsorption-desorption methodology, conducted on a BET surface analyzer at 77K.

2.2.3 Experimental protocol: Batch-wise adsorption

The reaction mixture was prepared by addition of Nickel nitrate Ni(NO₃)₂, Copper nitrate Cu(NO₃)₂ and Lead nitrate Pb(NO₃)₂ containing 20 ppm, to compute the adsorption behavior of ZnO-NPs at room temperature. The batch adsorption studies for Cu²⁺ ions removal with ZnO-NPs were conducted. In this respect, several physiochemical factors including pH, contact time, initial concentration and adsorbent quantity were studied to investigate the optimal adsorption behavior of ZnO-NPs as shown in table.1.

Table.1 Physiochemical parameters and analytical conditions

Physiochemical Parameters	Experimental Conditions
pH values	2.0, 3.0, 4.0, 5.0,6.0,7.0
Contact time	20, 60, 10, 20, 30,50, 70, 160
Initial metal ions concentration (mg/L)	10, 20, 30,40,60,80,100,150, 200, 300,500
Adsorbent dosage (mg)	3.0, 5.0, 8.0, 10.0, 15, 20, 30

The prepared solution pH value was adjusted by adding 0.1M HCl or NaOH strength solution. Adsorption behavior of prepared solution was measured at equilibrium state, wherein; supernatant suspension solution was discarded through 0.22µm filter membrane and calibrates

the Cu^{2+} ions concentration using the Flame atomic absorption spectroscopy (Perkin Elmer, 900F USA). Until adsorption process was achieved an equilibrium, Cu^{2+} ions adsorption capacity (Q_e , mg/g) and efficiency (η) were determined with the help of equation (1) and (2), respectively.

$$Q_e \left(\frac{\text{mg}}{\text{g}} \right) = \frac{(C_i - C_{eq})V}{m} \text{EQ. (1)}$$

$$(\eta, \%) = \frac{(C_i - C_{eq})}{C_i} \times 100\% \text{EQ. (2)}$$

Whereas; C_i , C_{eq} are initial and equilibrium concentration of copper Cu^{2+} ions (mg/l), (V) volume of copper Cu^{2+} cationic solution (L) and (m) the weight of ZnO-NPs (gms), respectively.

2.2.4 Statistical Analysis

All the experimental procedures were conducted in a triplicate manner and obtained data were analyzed. Other than this, the research data of adsorption capacity and efficiency were subjected to analyze significantly by means of one-way ANOVA in SPSS statistical *vers.*21 software ($p \leq 0.05$).

2. Results and Discussion

3.1 ZnO-NPs characterization

The powered XRD pattern results estimate the phase purity and crystallographic structure of synthesized ZnO-NPs. Notable diffraction peaks were observed at 31.62° , 34.34° , 36.23° , 47.63° , 56.64° , 62.94° , 67.91° and 69.04° , corresponding to the crystal planes (1 0 0), (0 0 2), (1 0 1), (1 0 2), (1 1 0), (1 0 3), (2 0 0), (1 1 2), (2 0 1), (0 0 4) and (2 0 2). The obtained results were found consistent with the standard data relevant to hexagonal ZnO crystal structure as already enlisted in the ICDD card (Jatoi et al. 2019) [17]. The highest intensity peaks shown in figure 1(a), confirms the well-graded crystalline three-dimensional structure of the synthesized Zn-NPs. Notably, no additional peaks were observed in the XRD patterns, indicating the synthesis of pure ZnO-NPs could occur when the low-temperature hydrothermal method was utilized, as depicted in figure 1 (a).

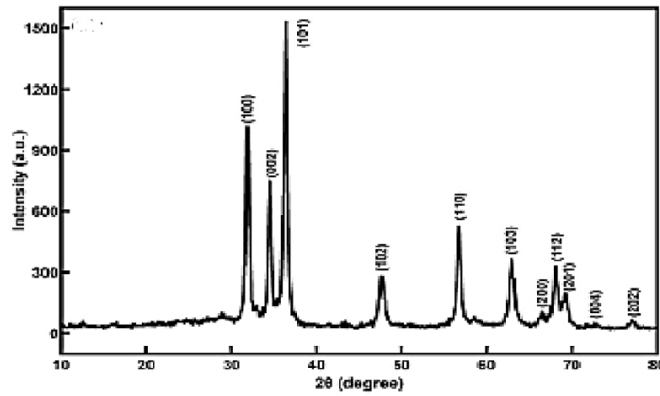


Fig.1 (a) Powered XRD diffraction pattern graph

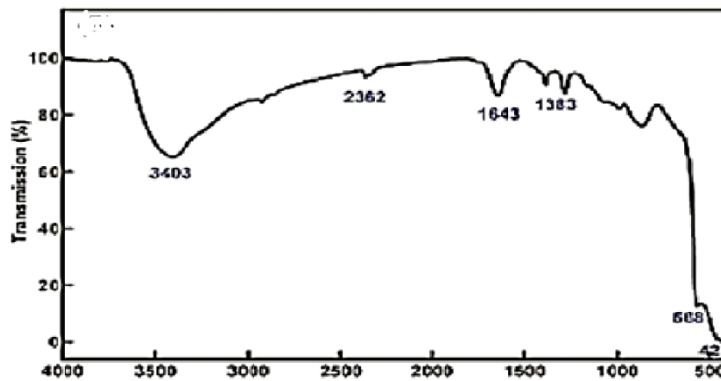


Fig.1 (b) FT-IR Spectral graph

A shown fig (1b) FT-IR spectrum depicts alteration in the chemical functional groups and chemical composition of ZnO-NPs. The shown spectra reflect the ZnO-NPs peaks at different 3403cm^{-1} , 2362cm^{-1} , 1643cm^{-1} , 1383cm^{-1} , 568cm^{-1} and 423cm^{-1} wave number, respectively.

The absorption peaks at 3403cm^{-1} correspond to O-H stretching vibration while band pattern at 1643cm^{-1} and 1383cm^{-1} were related to the bending mode of H_2O , originated from adsorption in the air as it was discussed earlier by Saravanakumar et al. (2019) [18].

The characteristic peaks at 2362cm^{-1} exhibit the asymmetric stretching of bonds and the CO_2 adsorption onto the zinc oxide (ZnO)-NPs surface as determined by Sharifalhoseini et al. (2015) [19]. However, the highlighted adsorption bands at 428cm^{-1} and 568cm^{-1} support the stretching vibrations of Zn-O bonding (He et al. 2019) [20]. Additionally, N_2 adsorption-desorption method display the specific surface area and porous structures development on ZnO-NPs.

Shown fig 2 (a, b) SEM images related to the presence of ZnO-NPs mesoporous structure and slit hole growth. The constructed isotherm typically shown in fig 1 (c) is IV-type manner with H_3 hysteresis loops.

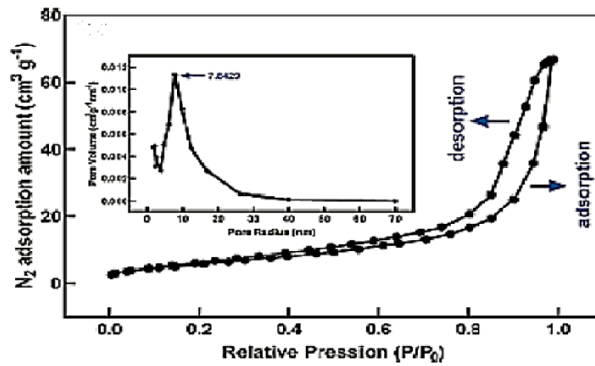


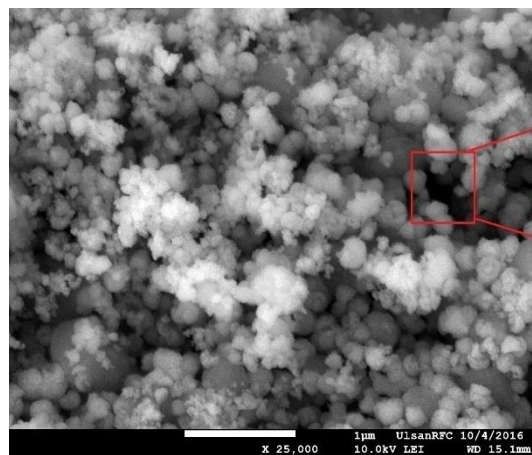
Fig.1 (c) Pore size distribution in ZnO-NPs and N₂-desorption-adsorption isotherm

Moreover, the calibrated BET specific surface area of ZnO-NPs was 26.777 m²/g, and measured surface area was found much larger than those of average size of ZnO-NPs as it follows Zheng et al. (2018) prescribed methodology [21]. The average pore volume and pore size were 0.104 ml/g and 7.8429 nm, which were found smaller compared to the current studied results. These physiochemical properties calibrations follow the Barret-Joyner-Halenda (BJH) methodology.

The surface area and mesoporous structural properties typically have a significant role in a cleanup of heavy metal ions as stated by Sharifalhosseini et al. (2015). Besides this, Fig. 2 SEM images represent the alteration in the surface textural and ZnO-NPs chemistry before and after reaction with copper ions. Shown Fig. 2(a) SEM images illustrate the ZnO-NPs spherical shape and a significant micro-porous structure before reacting to copper ions as this is typically a prime indicator particularly in the chemi-adsorption processes.

Whereas, ZnO-NPs interspaces show denser behavior as their surface is covered with a Cu²⁺ ions without affecting the physiological behavior of ZnO-NPs that was found close conformity with Mahdavi et al. (2012) studied results [22]. Furthermore, the ZnO-NPs EDX spectra (Fig. 2b) showing (3.89% weight percentage and 3.57% atomic percentage), which confirm the good adsorption of Cu²⁺ ions as these results represent the proper interaction of ZnO-NPs with Cu²⁺ ions. However, this experimental work purely defines the ZnO-NPs has a property to uptake Cu²⁺ ions significantly from industrial waste water stream compared to other prominent heavy metal ions including Ni²⁺, Pb²⁺, Cr³⁺

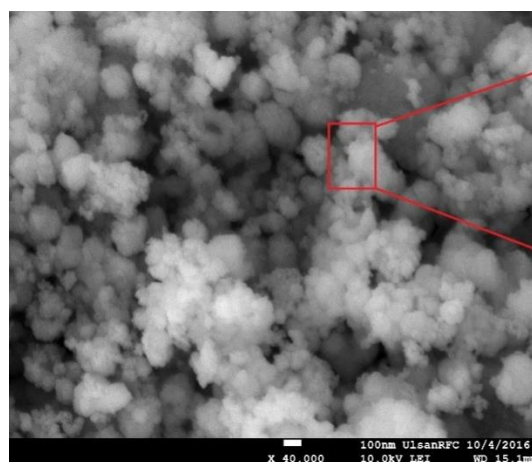
Before Adsorption		
Element	Weight %	Atomic %
O K	22.17	53.79



Before Adsorption of ZnO-NPs

Zn L	77.83	46.21
Totals	100.00	

Fig 2(a)

After adsorption of Cu²⁺ ion on ZnO-NPs

After Adsorption		
Element	Weight %	Atomic %
O K	11.65	34.76
Zn L	84.46	61.67
Cu K	3.89	3.57
Totals	100.00	

Fig 2(b)

Fig.2 (a) SEM-EDX spectra of ZnO-NPs before adsorption and Fig.2 (b) SEM-EDX spectra of ZnO-NPs after adsorption of copper ions.

3.2 ZnO-NPs sensitivity towards metallic ions

Four dominantly exists heavy metal ions including Ni²⁺, Pb²⁺, Cr³⁺ and Cu²⁺ were assessed in this study and all the relevant data were shown in fig 3. Shown fig 3 data represent the adsorption at 19.95 mg/g adsorption capacity and percentage recovery (99.77%) from the contaminated solution, which showed higher affinity towards Cu²⁺ ions. It was concluded a significant greater recovery of Cu²⁺ ions than the other three respective metal ions (P < 0.05).

In this respect, the different adsorption measurement may be co-related to the physicochemical property of studied metal ions (Le et al. 2019; Bora and Dutta, 2019) [23,24]. Actually, ZnO-NPs contain –OH- group, that is responsible for entangle heavy metal ions on its surface but this kind of interaction follows the complementary acid and base lewis principle suggested by CK, (1975)

[25]. This principle is more preferable to Cu^{2+} ion compared to Ni^{2+} , Pb^{2+} and Cr^{3+} ions. Thus, Cu^{2+} ion removal was found highly selective and prominent for further physiochemical study.

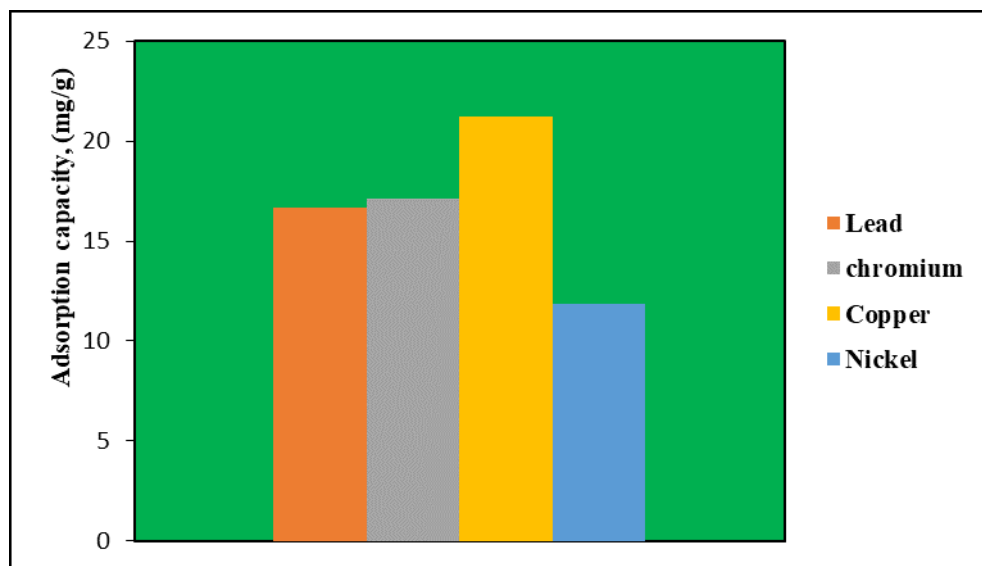


Fig.3 Heavy metal ions (Cu^{2+} , Ni^{2+} , Pb^{2+} , Cr^{3+}) adsorption screening on ZnO-NPs surface

3.3 pH effect on adsorption capacity

In the adsorption experiment, change in pH values affects the adsorbent surface charges and the degree of ionization of metal ions which ultimately predict the adsorption capacity of adsorbent. In this study adsorption capacity determination was carried out at different pH typically at (2.0-7.0) values on account of copper ion precipitation, which significantly predominantly shown at $\text{pH} \geq 6$ as discussed by Bagheri et al., (2014) compared to other metal ions [26].

Shown figs 4 reflect the pH effect on adsorption capacity of heavy metal ions on ZnO-NPs surface was evaluated. The maximal removal of (Cu^{2+}) ions is strongly dependent on the pH wherein; it observed that percentage removal of (Cu^{2+}) ions is actually happen at $>90\%$ relatively higher humid condition at $\text{pH} > 3$, which means maximal adsorption of copper ion would occur on ZnO-NPs at pH 3-4 range. Thus, with increment in the pH value to neutral pH promotes adsorption phenomenon because when solution pH reached closer to $\text{pH}=7$; initiates the more activation of hydroxylated active sites on to the ZnO-NPs surface for positive metallic ion especially selective to Cu^{2+} ions. As per our results, it was observed that $\text{pH} \geq 5$ reduce the adsorption frequency of ZnO-NPs because it forms a coordination complex with metal ions and hindered adsorption phenomenon on to ZnO-NPs surface. Henceforth, this experiment data

concluded that the effective adsorption of Cu^{2+} ions on to ZnO-NPs surface was occurred at pH 4 value which is valuable for further research work.

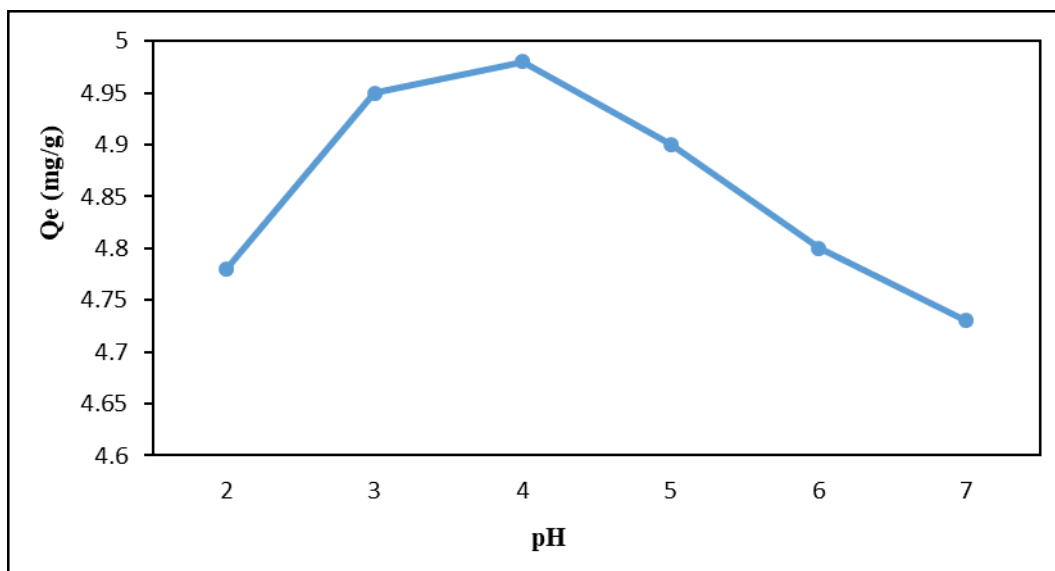


Fig.4 pH effect on Cu^{2+} ions adsorption on ZnO-NPs surface

3.4 Adsorption behavior kinetics and contact time effect

Shown figure (5) represent the contact time affect on metallic ion adsorption percentage at particular reaction time at fixed pH 4. Actually, metal ions adsorption capacity would depend on the available active sites on ZnO-NPs and indirectly interlinked to the contact time of metal ions on to the ZnO-NPs surface.

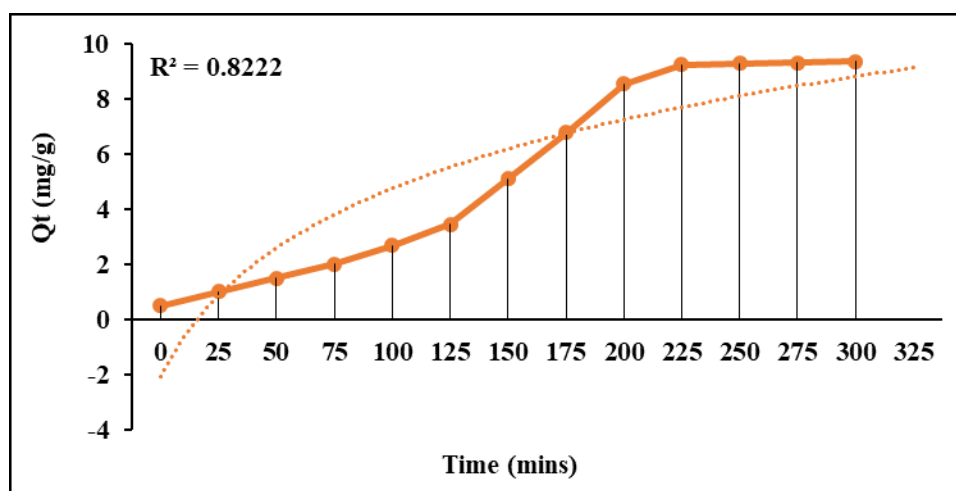


Fig. 5 Amount of Cu^{2+} ion removal using ZnO-NPs as adsorbent

Shown fig.5 describes the time variable influence on Cu^{2+} ions adsorption illuminate a consistent increment in Cu^{2+} ions adsorption onto ZnO-NPs surface would occur when the 50mg/ l of ZnO-NPs was utilized at 25 mins to 225 mins. As per shown fig.5 ZnO-NPs adsorption capacity inconsistency is altered with time and it follow the pseudo-first order kinetic model. Each recorded experimental data was calibrated as per given equations (3) & (4):

$$\ln(Q_e - Q_t) = \ln Q_e - K_1 t \quad \text{EQ. (3)}$$

Whereas; $Q_t(\text{mg g}^{-1})$ is the amount of Cu (II) adsorbed at given time t (min); K_1 pseudo-first order adsorption rate constant (min^{-1}).

$$\frac{t}{Q_t} = \frac{1}{K_2} + \frac{t}{Q_e} \quad \text{EQ. (4)}$$

Where K_2 (g/mg/min) is the pseudo-second-order adsorption rate constant.

The present study data showed the significant Cu^{2+} ion removal with the time and it achieves the equilibrium state at 225mins. Afterwards, no significant change was observed in between the 225 to 300 mins time frame. In addition, fig.6 and table-2 results show the adsorption behavior, which support the pseudo-second-order kinetic instead of pseudo-first order kinetic, as it shows linear correlation coefficient relation ($r^2 \geq 0.99$) at all Cu^{2+} ions removal from solution at 25°C .

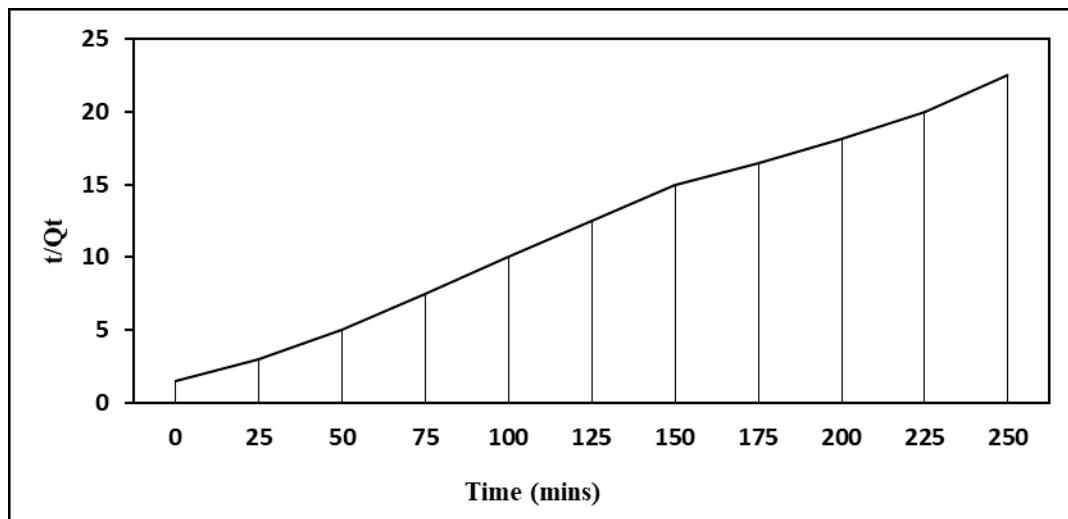


Fig.6 Evaluation of Cu^{2+} ion excluded amount per unit time

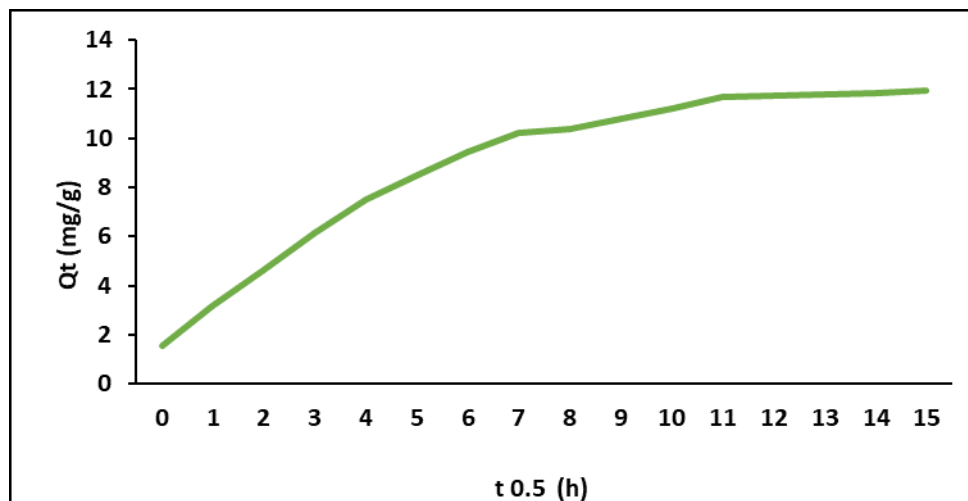
Table.2 Evaluation of Cu²⁺ ion exclusion kinetics parameters after ZnO-NPs adsorption

Sample (mg/g)	Q _e , exp	Pseudo first order kinetic				Pseudo second order kinetics		
		C _i (mg/L)	Q _e (mg/g)	10 ⁻² K ₁ h ⁻¹	r ² ₁	Q _e (mg/g)	10 ⁻² K ₁ h ⁻¹	r ² ₂
ZnO-NPs	9.88	50	6.78	2.64	0.822	9.83	1.53	0.997

This pseudo-second-order kinetic data are closer to the Q_e quantified data, thereby; encoded data revealed that adsorption phenomenon is actually correlated to the Cu²⁺ ion removal and available ZnO-NPs active sites as discussed by Almeida et al., (2010); and Jaerger et al., (2015) [27,28]. The encoded results were found in line with the Rafiq et al. (2014) and Kumar et al. (2013) and they also worked on adsorption of metal ion on ZnO-NPs surface [29,30]. Furthermore, an intra-particle diffusion analysis follows the approved Weber and Moris equation (5):

$$Q_t = K_{id} t^{0.5} + C_t \quad \text{Eq. (5)}$$

Whereas; K_{id} is the rate constant (mg g⁻¹ t^{-0.5}) and values of C_t defines the thickness of the boundary layer. However, K_{id} calibration would be essential when the graph between Q_t vs. t^{0.5} is plotted which follows the intra-particle diffusion based adsorption phenomenon.

**Fig.7 Intra-particle diffusion analysis of Cu²⁺ ion adsorption on ZnO-NPs surface**

Shown(fig.7) represent the Cu²⁺ ion removal using zinc oxide nanoparticle, as cupric ion removal is easily comprehensible through the intra-particle diffusion model.

The linear curvature in (fig.7) illustrates the adsorption of Cu²⁺ ion by ZnO-NPs which display adsorption at available active sites of zinc oxides surface. Subsequently, intra-particle diffusion

begin to decline and reached to plateau state when the maximal adsorption have been achieved on the adsorption site of oxide surface or it depend on the lowered metal ion concentration (Rafiq et al., 2014; Jaerger et al., 2015). This intra-particle diffusion mechanism is initially regulated by the external mass transfer and subsequently controlled during intra-particle diffusion until it reached to equilibrium state (Almeida et al., 2010; Jaerger et al., 2015). In addition, at initial stage, degree of diffusion rate constant (K_i) is greater than the equilibrium state (K_e) as thickness increment of adsorbent surface is frequently raised (Rafiq et al., 2014), as shown in table.3.

Table.3 Intra-particle diffusion analysis for Cu^{2+} ion adsorption on ZnO-NPs

Sample	Ci_1 (mg/L)	$10^{-2}K_{id1} \text{ h}^{-1}$	r^2_{1id}	Ci_2 (mg/L)	$10^{-2}K_{id2} \text{ h}^{-1}$	r^2_{2id}
ZnO-NPs	0.291	0.916	0.990	7.98	0.120	0.999

3.5 Effect of Metal Ion Concentration

Shown fig.8 represents the Cu^{2+} ion removal percentage that is influenced by the initial metal concentration. The effect of metal ion concentration was conducted at 25°C for 250 mins.

The present study results illustrate the Cu^{2+} ion removal percentage, initially at low metal ion concentration, metal adsorption phenomenon will occur very easily on the ZnO-NPs surface. However, the Cu^{2+} ion accumulation causes saturation of ZNO-NPs available active sites, which leads to a hindrance in metal exchange (Rafiq et al., 2014). Other than this, quick adsorption of Cu^{2+} ions on to a ZNO-NPs surface, indicate selectively higher adsorption capacity of ZnO-NPs for Cu^{2+} ions, which leads to a steady increment in copper adsorbed per gram of adsorbent (Q_e).

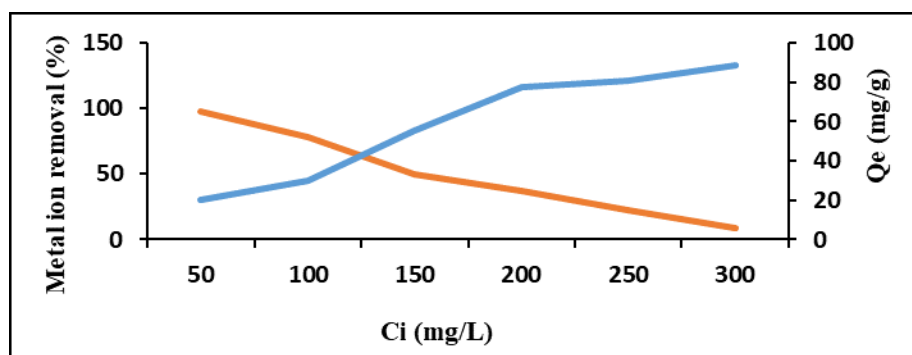


Fig.8 Initial metal ion concentration (Cu^{2+} removal) effect (C_i mg/L) on adsorption and equilibrium Q_e , (mg/g) status of ZnO-NPs surface

3.6 Effect of adsorbent dosage

Adsorbent dosage plays an important role in the heavy metal ion uptake. Different dosage of ZnO-NPs was applied onto (pH-4) 10ml Cu^{2+} solution. Shown fig.9 reflects the adsorption capacity calibration. Fig.9 shows increment in 17.67 mg/g to 19.93 mg/g adsorption capacity, which raised efficacy from 88.37% to 99.63% respectively, as the amount of ZnO-NPs is raised from 3mg to 10mg, create sufficient adsorption sites for Cu^{2+} ions.

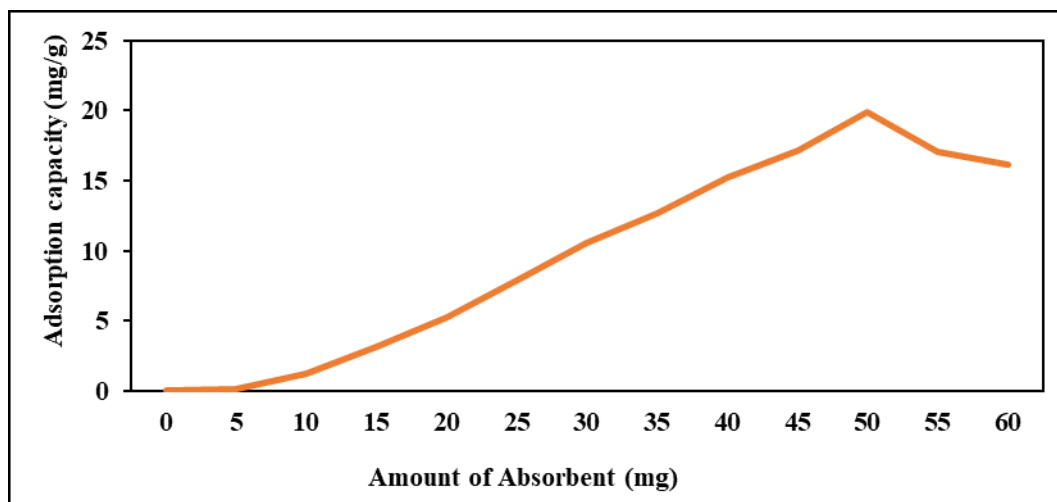


Fig.9 Effect of adsorbent (mg) amount on adsorption capacity of ZnO-NPs

However, increment in adsorption capacity and their efficacy as adsorbent dose is increases from 10mg to 50 mg as shown in fig.9, and these results were found in line with the Kera et al. (2017) results [31]. A 10.0mg desired dose of adsorbent per 10 ml (*i.e.*, 1g/l) was recorded as the minimum adsorbent dose, that was required to efficient Cu^{2+} ions removal from waste water streams.

3. Conclusion

This study focused on the synthesis of ZnO-NPs using the hydrothermal method and conducted a thorough characterization using XRD, FTIR, SEM-EDX, and BET-specific surface area analysis. The adsorption behavior of ZnO-NPs was investigated with respect to various physicochemical factors, including pH levels, adsorbent dosage, contact time, initial metal ion concentration, and the presence or absence of heavy metal ions. The research findings clearly demonstrate that the synthesized ZnO-NPs exhibit a remarkable affinity for Cu^{2+} ions compared to other heavy metal ions. The highest adsorption capacity of ZnO-NPs for Cu^{2+} ions was observed within a broad pH

range of 3-7, utilizing an adsorbent dosage of 1 g/L, a contact time of 250 minutes, and an initial Cu^{2+} concentration of 10 mg/L in aqueous solutions. Furthermore, the adsorption process followed pseudo-second-order kinetics, with ZnO-NPs achieving an impressive maximum removal efficiency of 89.56 mg/g for Cu^{2+} ions under the optimized conditions, surpassing the performance of other adsorbent materials. In summary, this study concludes that ZnO-NPs possess selective capabilities for the removal of positively charged heavy metal ions, making them a promising and sustainable solution for purifying industrial wastewater streams, representing an innovative approach in waste water purification strategies.

4. References

- i. Ali, R. M., Hamad, H. A., Hussein, M. M., and Malash, G. F. (2016). Potential of using green adsorbent of heavy metal removal from aqueous solutions: adsorption kinetics, isotherm, thermodynamic, mechanism and economic analysis. *Ecol. Eng.* 91, 317-332. doi:10.1016/j.ecoleng.2016.03.015
- ii. He X, Yang DP, Zhang X, Liu M, Kang Z, Lin C, JiaN, Luque R. (2019). Waste eggshell membrane-templated CuO-ZnO nanocomposites with enhanced adsorption, catalysis and antibacterial properties for water purification, *Chem. Eng. J.* 369, 621-633. <https://doi.org/10.1016/j.cej.2019.03.047>.
- iii. Saleh, T. A. (ed.). (2017). *Advanced Nanomaterials for Water Engineering, Treatment, and Hydraulics*. Hershey, PA: IGI Global. doi: 10.4018/978-1-5225-2136-5.
- iv. Kushwaha, D., Verma, Y. (2017). Evaluation of antioxidant and free radical scavenging activity of *Tagetes patula*. *Annual Research & Review in Biology*. 13(6):1-8.
- v. Al-AbriM, Al-Ghafri B, Bora T, Dobretsov S, Dutta J, Castelletto S, Rosa L, Boretti A. (2019). Chlorination disadvantages and alternative routes for biofouling control in reverse osmosis desalination. *J. Clean Water* 2, 2.
- vi. Bandyopadhyay S. (2016). Sustainable Access to Treated Drinking Water in Rural India. *Rural Water Systems for Multiple Uses and Livelihood Security*, 203-227. <https://doi.org/10.1016/B978-0-12-804132-1.00009-3>. EPA, (2011). *Water Treatment Manual: Disinfection*. Wexford, Ireland: Environmental Protection Agency.
- vii. Fu F and Wang Q. (2011). Removal of heavy metal ions from wastewaters: a review. *J. Environ. Manage.* 92, 407-418. doi: 10.1016/j.jenvman.2010.11.011.
- viii. Negrea, A., Ciopec, M., Lupa, L., Muntean, C., and Negrea, P. (2008). Studies regarding the copper ions removal from wastewaters. *Chem. Bull.* 53, 93-97. doi: 10.1007/s13201-019-1100-z.
- ix. Dermentzis, K., Christoforidis, A., and Valsamidou, E. (2011). Removal of nickel, copper, zinc and chromium from synthetic and industrial wastewater by electrocoagulation. *Int. J. Environ. Sci.* 1, 697-710.
- x. Da, browski, A., Hubicki, Z., Podko´scielyny, P., and Robens, E. (2004). Selective removal of the heavymetal ions from waters and industrial wastewaters by ion-exchange method. *Chemosphere* 56, 91-106.
- xi. Kebria, M. R. S., Jahanshahi, M., and Rahimpour, A. (2015). SiO₂ modified polyethyleneimine-based nanofiltration membranes for dye removal from aqueous and organic solutions. *Desalination* 367, 255-264.
- xii. Rafiq, Z., Nazir, R., Shahwar, D., Muhammad Raza, M. S., and Ali, S. (2014). Utilization of magnesium and zinc oxide nano-adsorbents as potential materials for treatment of

- copper electroplating industry wastewater. *J. Environ.* 2, 642–651. doi: 10.1016/j.jece.2013.11.004.
- xiii. Wang X, Cai W, Liu S, Wang G, Wu Z, and Zhao H. (2013a). ZnO hollow microspheres with exposed porous nanosheets surface: structurally enhanced adsorption towards heavy metal ions. *Colloids Surfaces A Physicochem. Eng. Asp.* 422, 199-205. doi: 10.1016/j.colsurfa.2013.01.031.
- xiv. Talaiekhosani A, Banisharif F, Bazrafshan M, Eskandari Z, Chaleshtari AH, Moghadam AG. (2019). Mohammad Amani, Comparing the ZnO/Fe(VI), UV/ZnO and UV/Fe(VI) processes for removal of reactive blue 203 from aqueous solution, *Environ. Health Eng. Manage.* 6 (1): 27-39. <https://doi.org/10.15171/ehem.2019.04>.
- xv. Babu AT, Antony R (2019). Green synthesis of silver doped nano metal oxides of zinc & copper for antibacterial properties, adsorption, catalytic hydrogenation & photodegradation of aromatics, *J. Environ. Chem. Eng.* 7 (1): 102840. <https://doi.org/10.1016/j.jece.2018.102840>.
- xvi. Leiva E, Tapia C, Rodriguez C, (2021). Highly Efficient Removal of Cu(II) Ions from Acidic Aqueous Solution Using ZnO Nanoparticles as Nano-Adsorbents. *Water*, 13(21), 2960; <https://doi.org/10.3390/w13212960>.
- xvii. A.W. Jatoi, I.S. Kim, H. Ogasawara, Q.Q. Ni, Characterizations and application of CA/ZnO/AgNP composite nanofibers for sustained antibacterial properties, *Mater. Sci. Eng. C: Mater. Biol. Appl.* 105 (2019) 110077. <https://doi.org/10.1016/j.msec.2019.110077>.
- xviii. Saravanakumar R, Muthukumaran K, Selvaraju N. (2019). Enhanced Pb (II) ions removal by using magnetic NiO/Biochar composite. *Mater. Res. Express* 6 (10):105504. <https://doi.org/10.1088/2053-1591/ab2141>.
- xix. Sharifalhosseini Z, Entezari MH, Jalal R (2015). Direct and indirect sonication affect differently the microstructure and the morphology of ZnO nanoparticles: optical behavior and its antibacterial activity. *Ultrason. Sonochem.* 27 466-473, <https://doi.org/10.1016/j.ultsonch.2015.06.016>.
- xx. He X, Yang DP, Zhang X, Liu M, Kang Z, Lin C, Jia N, Luque R (2019). Waste eggshell membrane-templated CuO-ZnO nanocomposites with enhanced adsorption, catalysis and antibacterial properties for water purification. *Chem. Eng. J.* 369, 621-633, <https://doi.org/10.1016/j.cej.2019.03.047>.
- xxi. Zheng S, Hao L, Zhang L, Wang K, Zheng W, Wang X, Zhou X, Li W, Zhang L, (2018). Tea polyphenols functionalized and reduced graphene oxide-ZnO composites for selective Pb²⁺ removal and enhanced antibacterial activity. *J. Biomed. Nanotechnol.* 14 (7): 1263-1276, <https://doi.org/10.1166/jbn.2018.2584>.
- xxii. Mahdavi S, Jalali M, and Afkhami A. (2012). Removal of heavy metals from aqueous solutions using Fe₃O₄, ZnO, and CuO nanoparticles. *J. Nanoparticle Res.* 14, 846. doi: 10.1007/s11051-012-0846-0.
- xxiii. Le AT, Pung SY, Sreekantan S, Matsuda A, and Huynh DP (2019). Mechanisms of removal of heavy metal ions by ZnO particles. *Heliyon* 5:e01440. doi: 10.1016/j.heliyon.2019.e01440.
- xxiv. Bora AJ and Dutta RK, (2019). Removal of metals (Pb, Cd, Cu, Cr, Ni, and Co) from drinking water by oxidation-coagulation-adsorption at optimized pH. *J. Water Process Eng.* 31 <https://doi.org/10.1016/j.jwpe.2019.100839>.
- xxv. Ck J, (1975). Continuum effects indicated by hard and soft anti-bases (Lewis acids) and bases, *Top. Curr. Chem.* 56, 1-66.

- xxvi. Bagheri, M., Azizian, S., Jaleh, B., Chehregani, A. (2014). Adsorption of Cu(II) from aqueous solution by micro-structured ZnO thin films. *J. Ind. Eng. Chem.* 20, 2439–2446. doi: 10.1016/j.jiec.2013.10.024.
- xxvii. Almeida, C. A. P., Santos, A., Jaeger, S., Debacher, N. A., and Hankins, N. P. (2010). Mineral waste from coal mining for removal of azo dye from aqueous solutions. *Desalination* 264, 181-187. doi: 10.1016/j.desal.2010.09.023.
- xxviii. Jaeger, S., Dos Santos, A., Fernandes, A. N., and Almeida, C. A. P. (2015). Removal of p-nitrophenol from aqueous solution using brazilian peat: kinetic and thermodynamic studies. *Water, Air, Soil Pollut.* 226, 236. doi: 10.1007/s11270-015-2500-9.
- xxix. Kumar, K. Y., Muralidhara, H. B., Nayaka, Y. A., Balasubramanyam, J., and Hanumanthappa, H. (2013). Low-cost synthesis of metal oxide nanoparticles and their application in adsorption of commercial dye and heavy metal ion in aqueous solution. *Powder Technol.* 246, 125-136. doi: 10.1016/j.powtec.2013.05.017.
- xxx. Rafiq, Z., Nazir, R., Shahwar, D., Muhammad Raza, M. S., and Ali, S. (2014). Utilization of magnesium and zinc oxide nano-adsorbents as potential materials for treatment of copper electroplating industry wastewater. *J. Environ.* 2, 642-651. doi: 10.1016/j.jece.2013.11.004.
- xxxi. Kera NH, Bhaumik M, Pillay K, Ray SS, Maity A. (2017). Selective removal of toxic Cr (VI) from aqueous solution by adsorption combined with reduction at a magnetic nanocomposite surface. *J. Colloid Interface Sci.* 503, 214-228, <https://doi.org/10.1016/j.jcis.2017.05.018>.